NEURAL REGENERATION RESEARCH
October 2014, Volume 9, Issue 20
www.nrronline.org

Synergistic actions of olomoucine and bone morphogenetic protein-4 in axonal repair after acute spinal cord contusion

Liang Chen[1, 2], Jianjun Li[1, 2, 3], Liang Wu[4], Mingliang Yang[1, 2, 3], Feng Gao[1, 2], Li Yuan[5]

1 Capital Medical University School of Rehabilitation Medicine, Beijing, China
2 Department of Spinal and Neural Function Reconstruction, China Rehabilitation Research Center, Beijing, China
3 Center of Neural Injury and Repair, Beijing Institute for Brain Disorders, Beijing, China
4 Rehabilitation Center, Beijing Xiaotangshan Rehabilitation Hospital, Beijing, China
5 Department of General Surgery, China Rehabilitation Research Center, Beijing, China

Corresponding author:
Jianjun Li, M.D., Department of Spinal Cord Neurological Reconstruction, Beijing Boai Hospital, China Rehabilitation Research Center, Beijing 100068, China, lcrrc9@gmail.com.

doi:*10.4103/1673-5374.143431*
http:*//www.nrronline.org/*

Accepted: *2014-08-22*

Abstract

To determine whether olomoucine acts synergistically with bone morphogenetic protein-4 in the treatment of spinal cord injury, we established a rat model of acute spinal cord contusion by impacting the spinal cord at the T_8 vertebra. We injected a suspension of astrocytes derived from glial-restricted precursor cells exposed to bone morphogenetic protein-4 ($GDAs^{BMP}$) into the spinal cord around the site of the injury, and/or olomoucine intraperitoneally. Olomoucine effectively inhibited astrocyte proliferation and the formation of scar tissue at the injury site, but did not prevent proliferation of $GDAs^{BMP}$ or inhibit their effects in reducing the spinal cord lesion cavity. Furthermore, while $GDAs^{BMP}$ and olomoucine independently resulted in small improvements in locomotor function in injured rats, combined administration of both treatments had a significantly greater effect on the restoration of motor function. These data indicate that the combined use of olomoucine and $GDAs^{BMP}$ creates a better environment for nerve regeneration than the use of either treatment alone, and contributes to spinal cord repair after injury.

Key Words: *nerve regeneration; spinal cord injury; olomoucine; glial-restricted precursor-derived astrocytes; glial scar; cavity; axonal regeneration; neural regeneration*

Funding: *This work was supported by a grant from the 'Twelve Five-year Plan' for Science & Technology Research of China, No. 2012BAI34B02.*

Chen L, Li JJ, Wu L, Yang ML, Gao F, Yuan L. Synergistic actions of olomoucine and bone morphogenetic protein-4 in axonal repair after acute spinal cord contusion. Neural Regen Res. 2014;9(20):1830-1838.

Introduction

Following spinal cord injury, axons cannot regenerate effectively (Fry, 2001) owing to an inhibitory internal microenvironment (Tator, 1995; Wang et al., 2002; Tang et al., 2003; Kuerten et al., 2011). Numerous studies have been carried out with the aim of facilitating axonal regeneration following spinal cord injury (Akpek et al., 1999; Sharp et al., 2010; Park et al., 2011; Bazley et al., 2012; Han et al., 2012; Hill et al., 2012; Ozdemir et al., 2012; Wiliams and Bunge, 2012; Yazdani et al., 2012; Fan et al., 2013; Piao et al., 2013), with little success. Axonal regeneration is a complicated process controlled by various factors (Davies et al., 1997; Akpek et al., 1999; Bramlett and Dietrich, 2007). In normal spinal cord tissue, mature astrocytes maintain the morphology of neurons and provide vital nerve growth factors (Giménez y Ribotta et al., 2001). However, excessive proliferation of glial cells after spinal cord injury leads to the formation of glial scars (Shechter et al., 2011; Parry and Engh, 2012), which secrete harmful factors, such as chondroitin sulfate proteoglycans. Furthermore, after spinal cord injury, a cavity is formed (Kakulas, 1987; Tator, 1995). Glial fibers surrounding the cavity begin to grow in a disorderly manner (Davies et al., 2006). Together, the cavity and dense, disordered glia constitute a physical and chemical barrier to axonal regeneration (Hobohm et al., 2005; Wu et al., 2012). Therefore, to repair spinal cord damage, combination therapy is necessary to suppress glial cell proliferation and reduce the size of the cavity.

Olomoucine (2-(2-hydroxyethylamino)-6-benzylamino-9-methylpurine) is a purine derivative that competitively inhibits the activity of cyclin-dependent kinase (CDK) 1, CDK2 and CDK5 *in vitro*. The molecule binds to the enzymes' adenosine triphosphate binding sites and inhibits interactions between CDK1 and cyclin B, CDK2 and cyclin E or A, as well as the activity of extracellular signal-regulated kinase 1 or mitogen-activated protein (Glab et al., 1994; Morgan, 1995). Inhibition of CDK interrupts the cell cycle at the G_1/S and G_2/M checkpoints, and blocks DNA synthesis and cell division (Fan et al., 1999; Arris et al., 2000). Olomoucine inhibits glial proliferation and glial scar formation in the spinal cord after injury, and reduces inhibitory factors; thus, it may improve the microenvironment of the injury

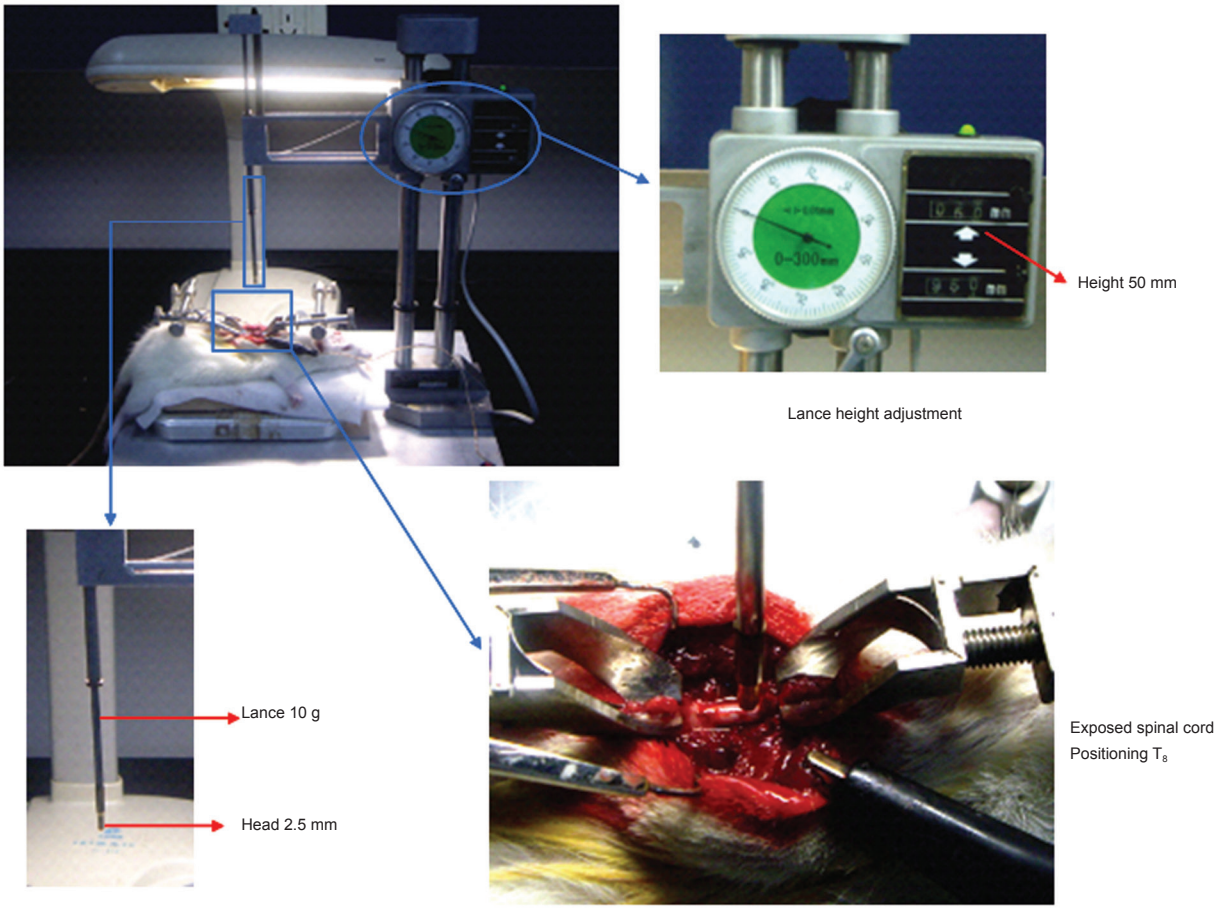

Figure 1 Equipment and method for establishing a model of spinal cord injury.
Spinal cord contusion at T_8 was carried out by dropping a weight of 10 g onto the spinal cord from a height of 50 mm.

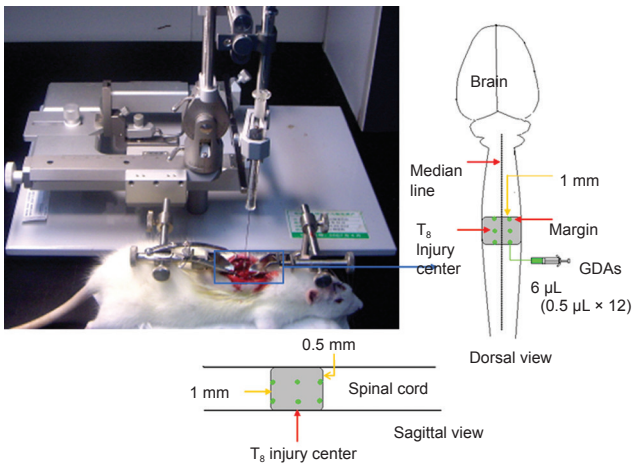

Figure 2 Cell transplantation in rats after T_8 spinal cord contusion.
Glial-restricted precursor-derived astrocytes induced by bone morphogenetic protein-4 (GDAs^{BMP}) were transplanted at 12 injection sites. Dorsal view: The six entry points (green) for cell transplantation. Sagittal view: the three rostrocaudal levels and two depths at which cells were injected (green).

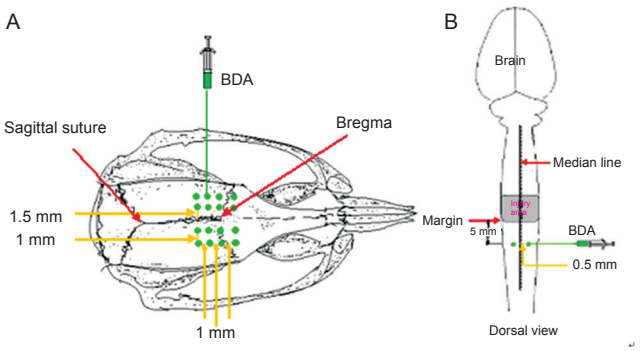

Figure 3 Anterograde axon tracing for biotinylated dextran amine (BDA).
(A) Anterograde motor axon tracing: 16 injection sites (green) in the motor cortex. (B) Anterograde sensory axon trace: two injection sites (green) on the dorsal spinal cord approximately 5 mm caudal to the injured area.

zone for axonal regeneration (Tian et al., 2006).

Glial-restricted precursor cells are the precursors of oligodendrocytes and astrocytes. When induced by bone morphogenetic protein-4, they develop into a novel population of glial-restricted precursor cells-derived astrocytes (GDAs^{BMP}) with unique properties (Gregori et al., 2002; Liu et al., 2002; Phillips et al., 2012). When transplanted into injured spinal cord, GDAs^{BMP} fill the injury cavity, moderately inhibit glial scarring, realign host tissues, and delay the expression of inhibitory proteoglycans (Davies et al., 2006). Furthermore, GDAs^{BMP} can also significantly reduce axonal atrophy in the central nervous system (Davies et al., 2006). Together, this

evidence suggests that GDAs^{BMP} may be highly effective in the repair of the damaged spinal cord (Davies et al., 2006).

Therefore, in the present study, we investigated the separate and combined effects of olomoucine and GDAs^{BMP} in rats with T_8 contused spinal cord, using behavioral and histochemical techniques.

Materials and Methods

Animals

A total of 72 healthy adult female specific-pathogen-free Sprague-Dawley rats, aged 6 weeks and weighing 200 ± 10 g, were provided by the Experimental Center of the Academy of Military Medical Sciences in China (License No. SCXK (army) 2007-004). All rats were housed at 23°C and relative humidity of 50%. The protocols were approved by the Rehabilitation Medical Ethics Committee, Capital Medical University, China. All rats were randomly divided into four groups: model (control), olomoucine, GDAs^{BMP}, and olomoucine + GDAs^{BMP}.

Preparation of spinal cord contusion model

Animals were anesthetized with an intraperitoneal injection of 1% sodium pentobarbital (35 mg/kg). Approximately 5 mm of spine was exposed at T_8, and spinal cord contusion was performed using the New York University impactor device, with a weight of 10 g dropped onto the spinal cord from a height of 50 mm. The contusion model was considered successful when the hind legs and tail twitched spastically several times until flaccid paralysis occurred (Anderson et al., 2004) (**Figure 1**).

Cell and drug treatment

GDAs^{BMP} were transplanted into the injured spinal cord in the GDAs^{BMP} and olomoucine + GDAs^{BMP} groups. GDAs^{BMP} cell suspension (30,000/μL; Sigma-Aldrich, St. Louis, MO, USA) was injected into the T_8 segment of the spinal cord immediately after injury, using a micro-syringe fixed on a stereotaxic frame (Zhenghua Biological Equipment Co., Ltd., Huaibei, Anhui Province, China). Twelve injection sites were used, each receiving 0.5 μL: two points 0.5 mm either side of the posterior median sulcus, placed at three levels along the spinal cord (at the center of the injury, 1 mm rostral to the injury, and 1 mm caudal to the injury), and each at two depths (0.5 mm and 1.5 mm) (**Figure 2**). The needle was inserted first to 1.5 mm depth; the cells were slowly injected, and the needle was maintained in place for 1 minute. The needle was then pulled out to 0.5 mm depth, and maintained in place for 10 minutes, before being removed completely. Finally, the wound was sutured. In the model and olomoucine groups, wounds were sutured immediately after the model had been established.

Thirty minutes and 24 hours after injury, rats in the olomoucine and olomoucine + GDAs^{BMP} groups were injected intraperitoneally with 4 mg/kg olomoucine (Alexis Biochemicals, San Diego, CA, USA) in physiological saline (80 mg/mL).

All rats were injected with penicillin (50,000 U/kg) for 3 days after surgery, and manual expression of the bladder was performed until autonomic micturition reflex appeared. Additionally, cyclosporin A (10 mg/kg intramuscularly) was administered to rats that had received GDAs^{BMP}.

Evaluation of behavior using the Basso Beattie Bresnahan Locomotor Rating Scale

The behavior of rats in each group was observed at 3, 7, 14, 21 and 28 days after surgery. The Basso Beattie Bresnahan scale was used to evaluate hind limb motor function (Basso et al., 1995). Nine indexes were observed: body movement; trunk and abdomen position; trunk stability; front and hind limb coordination; gait; paw action; paw rotation; toe position; tail position. The hind limb motor functions of the rats were divided into 22 levels, in which a score of 0 indicated panplegia and a score of 21 indicated normal movement. Because a full bladder may affect locomotor activity, artificial micturition was carried out 1 hour before evaluation.

Anterograde tracing of motor and sensory axons with biotinylated dextran amine

Biotinylated dextran amine motor tracing was conducted 2 weeks before the rats were sacrificed. Rats were anesthetized with 1% pentobarbital sodium (35 mg/kg intraperitoneally) and secured on a stereotaxic frame. Bregma and the sagittal suture were used as reference points (Ersahin et al., 2011). Holes were drilled into the skull to allow 16 cortical injection points: 1.5 and 2.5 mm lateral to the sagittal suture, bilaterally, at four rostrocaudal levels (1 mm rostral to bregma; bregma; 1 mm caudal to bregma; 2 mm caudal to bregma) (**Figure 3A**). A 10% solution of biotinylated dextran amine -10,000 (Molecular Probes, Eugene, OR, USA) was injected slowly into the cortex (0.5 μL per injection point; 0.1 μL/min) at a depth of 1 mm from the brain surface. The total volume of biotinylated dextran amine injected was 8 μL (**Figure 3A**).

Biotinylated dextran amine sensory tracing was conducted 1 week before the rats were sacrificed. Animals were anesthetized as described above, and secured in the stereotaxic frame. The spinal dura mater was exposed at the T_{10} vertebra. Biotinylated dextran amine solution (10%; 0.5 μL) was slowly injected (0.1 μL/min) into the spinal cord at two points: approximately 5 mm away from the caudal margin of the injury area, bilaterally (0.5 mm either side of the posterior median sulcus), at a depth of 0.5 mm (**Figure 3B**). The needle was maintained in place for 10 minutes before being withdrawn slowly.

Double-labeling immunohistochemistry

At 3, 7 and 28 days after surgery, six rats from each group were deeply anesthetized and perfused transcardially with 4% paraformaldehyde solution. The injured section of the spinal cord, 15 mm in length, was removed and fixed in 4% paraformaldehyde solution for 6 hours, before immersion in 30% sucrose/PBS overnight at 4°C. The tissue was embedded in optimal cutting temperature tissue freezing medium (Sakura, Tokyo, Japan) and serial sections (50-μm thick) were cut using a freezing microtome. According to the direction of the biotinylated dextran amine trace, the center of the injury was designated "0", and sections were taken at −1.5, −1, 0, +1,

+1.5 and +5 mm (where "–" represents the proximal end of the biotinylated dextran amine injection and "+" represents the distal end). Antigen retrieval was carried out by incubating the sections in sodium citrate buffer with 0.1% Triton X-100 for 10 minutes. All samples were then blocked with 5% standard goat serum for 30 minutes at room temperature, and incubated with rabbit anti-glial fibrillary acidic protein polyclonal antibody (1:100; Sigma-Aldrich) overnight at 4°C, followed by Avidin-Cy3 (1:50; Sigma-Aldrich) and goat anti-rabbit IgG-FITC (1:50; Zymed Laboratories Co., San Diego, CA, USA) for 2–3 hours at room temperature, and washed in PBS with 0.1% Tween 20. Tissue sections were placed under a fluorescence microscope (DMLA 4000B and TCS SP5 confocal; Leica, Wetzlar, Germany) to observe biotinylated dextran amine expression (Avidin-Cy3-labeled, red) and glial fibrillary acidic protein (IgG-FITC-labeled, green). Image-Pro Plus 6.0 software (Media Cybernetics, Rockville, MD, USA) was used to calculate integrated optical density values expressed by glial fibrillary acidic protein at 28 days after spinal cord contusion. A high integrated optical density value represents a severe degree of glial scarring. Cavity area and the angle between glial fibrillary acidic protein-immunopositive fibers in the injury region were also calculated using Image-Pro Plus. The angle represents the linear arrangement of fibers, with a small angle indicating good linearity for axonal growth and transport (Davies et al., 2006).

Statistical analysis

All data were expressed as the mean ± SD, and analyzed using SPSS 16.0 software (SPSS, Chicago, IL, USA). Intergroup comparisons were performed using one-way analysis of variance, and *t*-tests were used for pairwise comparisons. $P < 0.05$ was considered statistically significant.

Results

GDAs^{BMP} reduced lesion cavity size after spinal cord contusion

Double-immunohistochemistry revealed that a small cavity appeared shortly after spinal cord injury, and grew gradually, especially in the first 3–7 days. In the olomoucine group, the size of the cavity was not significantly different from that in the model group at any time point. However, in the GDAs^{BMP} transplantation group, no cavity was observed at 3 days after surgery, and at 7 days the cavity size was notably smaller than in the model and olomoucine groups ($P < 0.01$). The difference remained significant until the end of the experiment (28 days; $P < 0.05$). This suggests that GDAs^{BMP} prevent cavity formation in the early stages of spinal cord injury. In the olomoucine + GDAs^{BMP} group, the size of the cavity was not significantly different from that in the GDAs^{BMP} group, indicating that olomoucine does not influence the inhibitory action of GDAs^{BMP} on the cavity (**Figure 4**).

Olomoucine inhibited glial scar formation after spinal cord contusion

Double immunofluorescence did not reveal any significant differences in glial fibrillary acidic protein expression between the model and GDAs^{BMP} groups ($P > 0.05$), suggesting that the application of GDAs^{BMP} has no effect on glial scar formation after spinal cord injury. However, glial fibrillary acidic protein expression in both olomoucine-treated groups was significantly lower than in the model and GDAs^{BMP} groups ($P < 0.05$), with no difference between the olomoucine and olomoucine + GDAs^{BMP} groups ($P > 0.05$). This suggests that olomoucine effectively prevents astrocyte activation and gliosis, but that this effect is not strengthened by GDAs^{BMP} (**Figures 4**, **5**).

Effects of GDAs^{BMP} and/or olomoucine on glial fibrillary acidic protein-immunopositive fibers and biotinylated dextran amine-positive axons after spinal cord contusion

In the model group, 28 days after spinal cord injury, astrocytes in the damage zone had proliferated. Glial fibrillary acidic protein-immunopositive fibers were thick and branched, typical of compact scar tissue. However, after olomoucine intervention, gliosis was inhibited, and glial fibrillary acidic protein-immunopositive fibers were relatively sparse and thin, although the angles between them were still large and the fibers formed a dense mass. Morphological differences in biotinylated dextran amine-positive axons were observed between the two groups at the proximal end of the injury and included thinner or thicker axons, formation of neuromas, branching and sprouting, and bending or winding growth. A few biotinylated dextran amine-positive axons were seen at the center of the injury site (**Figure 6**).

In the GDAs^{BMP} group, 28 days after injury, compact scar tissue was visible in the damage zone, accompanied by some small regions where glial fibrillary acidic protein-positive fibers lay along the vertical axis of the spinal cord. These fibers had obvious linear characteristics and kept in line with the direction of the regenerated biotinylated dextran amine-positive neural fibers. The mean angle between glial fibrillary acidic protein-immunopositive fibers in this region was 29.66°, notably smaller than the 62.34° of reticular fibers ($P < 0.01$; **Figure 7**). However, the linear characteristics of most of the fibers in this region were lost at the scar border, so that the majority of accompanying biotinylated dextran amine-positive axons lost continuity. In the olomoucine + GDAs^{BMP} group, linear fibers and sparse reticular fibers coexisted in the damage zone. Glial fibrillary acidic protein-immunopositive fibers were more linear at the border, and biotinylated dextran amine-positive fibers passed through the cavity.

Effects of GDAs^{BMP} and/or olomoucine on Basso Beattie Bresnahan scores after spinal cord contusion

One day after injury, the Basso Beattie Bresnahan score in all animals was 0. On days 3 and 7 post-injury, the scores in each group improved considerably. In the GDAs^{BMP} and olomoucine + GDAs^{BMP} groups, Basso Beattie Bresnahan scores were higher than those in the model and olomoucine groups ($P < 0.05$). By 14 days, the rate of recovery slowed in the model and GDAs^{BMP} groups, so that the difference in Basso Beattie Bresnahan score between the olomoucine and GDAs^{BMP} groups was lost ($P > 0.05$, day 14); however, Basso

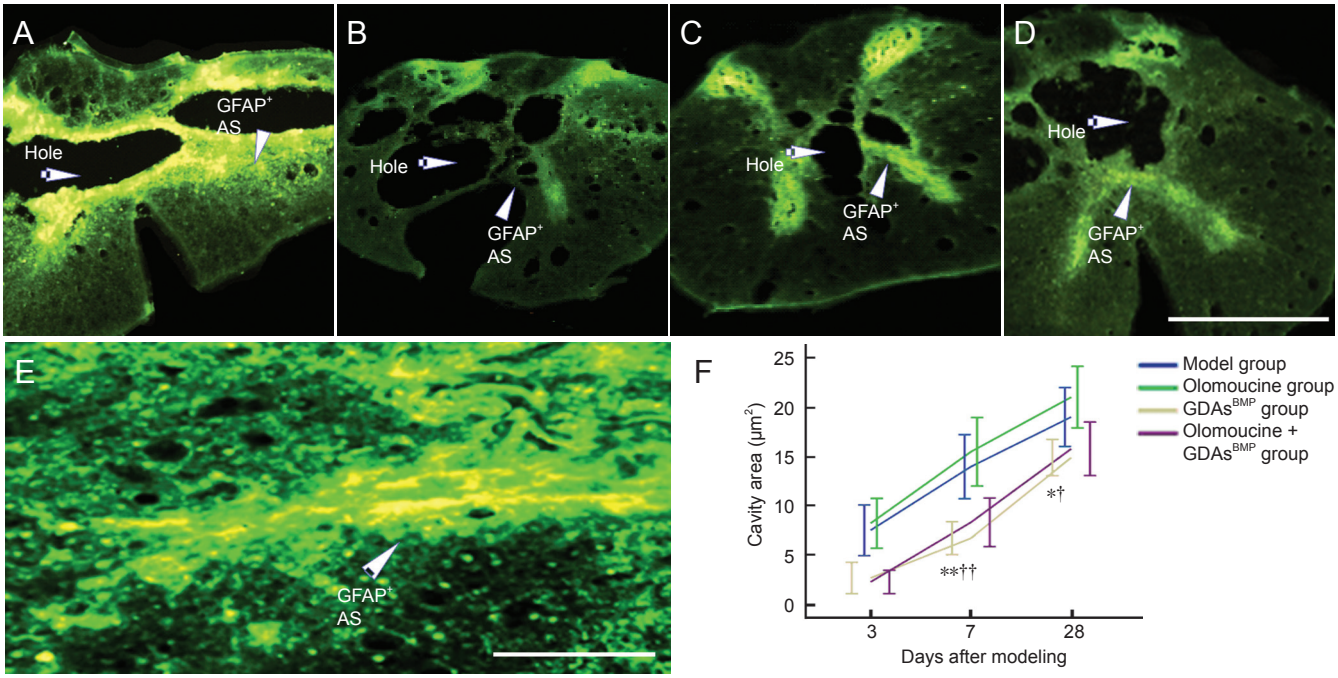

Figure 4 Astrocytes (AS) in rats with T_8 contused spinal cord after injury (immunohistochemistry) and effect of glial-restricted precursor-derived astrocytes induced by bone morphogenetic protein-4 ($GDAs^{BMP}$) and/or olomoucine on cavity formation.
(A) Model group: Large cavity (arrow) and dense scars (arrowhead); (B) olomoucine group: cavity size similar to that of the model group, but less glial scarring; (C) GDAsBMP group: smaller cavity than in model rats but dense surrounding scar; (D) olomoucine + $GDAs^{BMP}$ group: small cavity and little scarring; (E) longitudinal section of model group: dense scarring and disorganized fibers. Glial fibrillary acidic protein (GFAP), astrocyte marker; positive expression is labeled by IgG-FITC (green). Scale bars: (A–D) 2 mm; (E) 125 μm. (F) Effect of $GDAs^{BMP}$ and olomoucine on cavity area in the damage zone of rats with spinal cord contusion. Data are expressed as the mean ± SD; $n = 6$ rats per group. One-way analysis of variance was used for intergroup comparison; *t*-tests were used for pairwise comparisons. $*P < 0.05$, $**P < 0.01$, *vs.* model group; $†P < 0.05$, $††P < 0.01$, *vs.* olomoucine group.

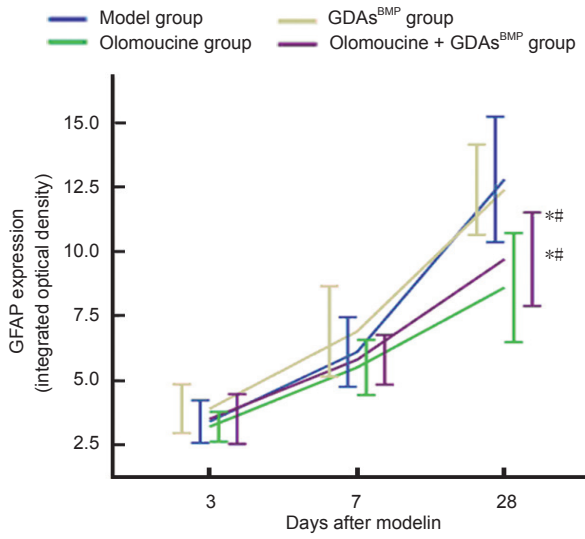

Figure 5 Effects of glial-restricted precursor-derived astrocytes induced by bone morphogenetic protein-4 ($GDAs^{BMP}$) and olomoucine on glial fibrillary acidic protein (GFAP) expression in the damage zone of the spinal cord in rats after spinal cord contusion.
Data are expressed as the mean ± SD; $n = 6$ rats per group. One-way analysis of variance was used for intergroup comparison; *t*-tests were used for pairwise comparisons. $*P < 0.05$, *vs.* model group; $\#P < 0.05$, *vs.* $GDAs^{BMP}$ group.

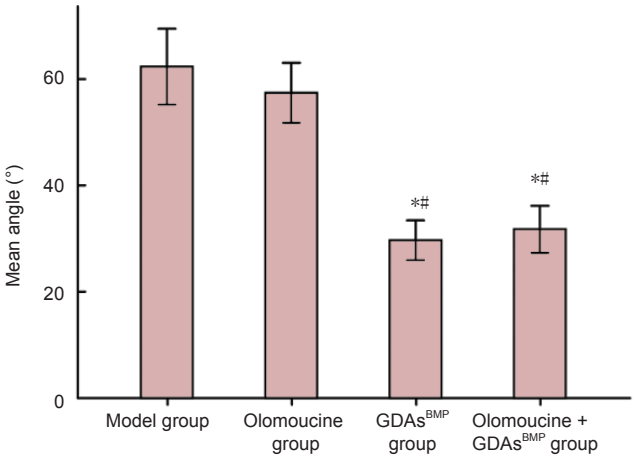

Figure 7 Effect of $GDAs^{BMP}$ and olomoucine treatment on angles between GFAP-immunopositive fibers in the damage zone in rats with T_8 contused spinal cord at 28 days after injury.
The angles between GFAP-immunopositive fibers in the damage zone represents the linearity among the fibers. The smaller the angle, the more linear the arrangement. A linear arrangement is beneficial for axonal growth across the lesion cavity. Data are expressed as the mean ± SD; $n = 6$ rats per group. One-way analysis of variance was used for intergroup comparison; *t*-tests were used for pairwise comparisons. $*P < 0.05$, *vs.* model group; $\#P < 0.05$, *vs.* $GDAs^{BMP}$ group. $GDAs^{BMP}$: glial-restricted precursor-derived astrocytes induced by bone morphogenetic protein-4; GFAP: glial fibrillary acidic protein.

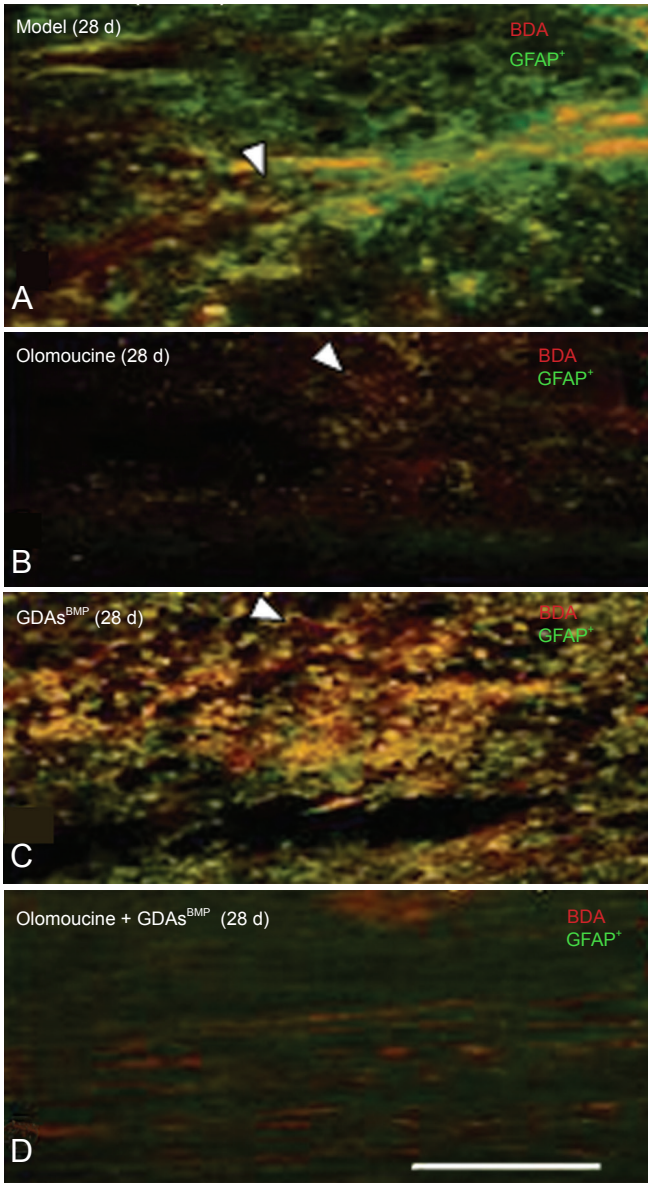

Figure 6 Longitudinal sections showing effect of GDAs^{BMP} and olomoucine treatment on GFAP-immunopositive fibers and BDA-positive axons in rats with T_8 contused spinal cord 28 days (d) after injury (double-fluorescence immunohistochemistry).
(A) Model group: Disorganized fibers and dense scar tissue in the damage zone; BDA-positive axons were curved and winding at the injury margin (arrow). (B) Olomoucine group: Light scarring but large cavity; BDA-positive axons thick and clustered in some parts, forming a neuroma (arrow). (C) GDAs^{BMP} group: Dense scarring at the injury border; some linearly-arranged BDA-positive axons (arrow) passing through cavity. (D) Olomoucine + GDAs^{BMP} group: GFAP-immunopositive positive fibers and BDA-positive fibers in linear array with high correlation. GFAP (astrocyte marker) labeled with FITC (green). BDA (axonal regeneration marker) labeled with Avidin-Cy3 (red). GDAs^{BMP}: Glial-restricted precursor-derived astrocytes induced by bone morphogenetic protein-4; GFAP: glial fibrillary acidic protein; BDA: biotinylated dextran amine.

Beattie Bresnahan scores remained greater in the olomoucine and GDAs^{BMP} groups than in the model group ($P < 0.05$), and in the olomoucine + GDAs^{BMP} group than in the olomoucine and GDAs^{BMP} groups ($P < 0.05$). After day 14, no further changes in Basso Beattie Bresnahan score were observed in any group except the olomoucine + GDAs^{BMP} group, in which Basso Beattie Bresnahan score improved until the end of the 28-day observation period, and remained significantly different from the other groups ($P < 0.05$; **Figure 8**).

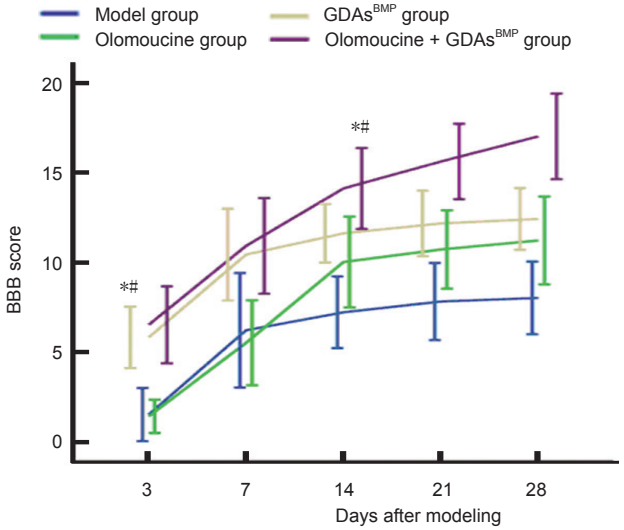

Figure 8 Effects of glial-restricted precursor-derived astrocytes induced by bone morphogenetic protein-4 (GDAs^{BMP}) and olomoucine treatment on behavior in rats with T_8 contused spinal cord at 28 days after injury.
Data are expressed as the mean ± SD; n = 18, 12, 6, 6, and 6 at 3, 7, 14, 21, and 28 days, respectively. One-way analysis of variance was used for intergroup comparison; t-tests were used for pairwise comparisons. *$P < 0.05$, *vs.* model group; #$P < 0.05$, *vs.* GDAs^{BMP} group. BBB: Basso Beattie Bresnahan locomotor score.

Discussion

Following spinal cord injury, the earliest change in histology is bleeding, which may result from the rupture of the thin-walled vessels in the central gray matter (Gao et al., 2013; Liu et al., 2013a; Zhao et al., 2013). Later, along with increased activity of polymorphonuclear leukocytes and gitter cells around the bleeding vessels, the cells release large amounts of inflammatory mediators (Xu and Cheng, 2013; Zhang et al., 2013). The permeability of the vascular wall is increased, causing a secondary reaction. The injury area grows and stimulates glial activation (Huang et al., 2013; Liu et al., 2013b). Glia proliferate widely within the region of damage, and start to constitute the dense scar tissue together with the extracellular matrix (Bunge, 2001; Seki et al., 2002), in which the cell processes become arranged in a grid. These scars form physical barriers that prevent axons from following their original growth path. Additionally, glia secret harmful factors, further impeding axonal growth through the damage zone. This results in bending or winding of the axon terminal, or the formation of neuroma, and a loss of contact with distal processes. For these reasons, prevention of glial scarring is very important in the treatment of spinal cord injury.

Olomoucine regulates the cell cycle of activated glial cells *in vitro* (Tian et al., 2006). In rats with spinal cord injury, administration of olomoucine inhibits the proliferation of gitter cells, reduces secondary reactions in the spinal cord

after injury, and decreases tissue edema and syringomyelia (Tian et al., 2007). We hypothesized that olomoucine would reduce the release of inflammatory mediators, thus impairing astrocyte activation, and regulate the astrocyte cell cycle, block proliferation, and ultimately inhibit the formation of scar tissue. However, we did not observe any notable differences between the olomoucine and model groups in glial fibrillary acidic protein expression, cavity area or Basso Beattie Bresnahan score 3 or 7 days after injury, suggesting that olomoucine has little effect in the early stages of injury.

A possible reason why olomoucine did not interfere in the glial cell cycle in the damaged spinal cord as expected may be because its action was delayed by the complex microenvironment in the damaged spinal cord, causing it to miss the microglial regulation window. Later, the size of the lesion depends on the degree of hemorrhagic necrosis and gliosis. Olomoucine-treated rats had larger cavities than rats in the other groups, because of the drug's gliosis-inhibiting function. However, the degree of inhibition was small, and not statistically significant.

From 14 days post-injury, Basso Beattie Bresnahan scores in the model group stabilized, whereas in the olomoucine group they continued to improve, suggesting that the drug somehow influences axonal repair at 7–14 days. Although immunohistochemistry was not performed at these time points, the results at 28 days show that olomoucine had significantly inhibited the formation of glial scars around the lesion cavity. Glial proliferation occurred in the damaged area from 7 days after injury. At this point, when a large number of astrocytes enter the proliferation cycle, stimulated by inflammatory factors, olomoucine may start to inhibit further activation. Thus, the growth of the glial scar, which secretes harmful factors, is inhibited, allowing more axons to grow through the damaged area and form synapses with the distal region, and facilitating the recovery of neural function. However, the extent of necrosis and size of the lesion cavity were not affected by olomoucine alone; various substances that inhibit production of gitter cells, myelin sheath formation, and axonal regeneration, may impair the restorative effect of olomoucine in spinal cord injury.

The lesion cavity is an important factor impeding neuroregeneration. It appears about 3 days after injury, initiated from coagulative necrosis in the center of the damaged spinal cord (Zhou and Li, 2006). Gitter cells start to proliferate, and digest and clear the necrotic tissues following the secondary reaction. A necrotic cavity is formed, increasing the area of spinal damage. When regenerative axons reach the proximal area of the cavity, they are unable to cross it because of a lack of supportive structures. However, in the present experiment, we observed that when GDAs^{BMP} were transplanted into the injured spinal cord, the cavity area was notably smaller at every time point from 3 days after surgery, compared with the model group. It has been shown *in vitro* that GDAs^{BMP} migrate to the injury site, proliferate, and fill the cavity (Kobayashi et al., 1997; Schucht et al., 2002). Furthermore, GDAs^{BMP} delay the expression of inhibitory proteoglycans, promote axonal regeneration of the tractus rubrospinalis, and inhibit neuronal atrophy in the red nucleus (Kobayashi et al., 1997; Schucht et al., 2002). They also secrete brain-derived neurotrophic factor, which is neuroprotective and prevents axonal atrophy (Davies et al., 2006). Thus, transplantation of GDAs^{BMP} into the damaged area provides not only a physical channel for axonal growth, but also a biochemical environment conducive to neuronal regeneration.

We also showed here that although GDAs^{BMP} are astrocytes, when induced by bone morphogenetic protein 4, their processes are characterized by distinct linear features during growth and differentiation after injury. That is, these cells grow along the vertical axis of the spinal cord, with small angles between processes and a staggered conformation. Our double-labeling fluorescence study shows that this linear arrangement correlates with the growth of neural fibers. Together, this evidence demonstrates that GDAs^{BMP} can bridge the lesion cavity and shorten the path of axonal growth, enhancing the efficiency of axons passing through the injury interface and thus promoting the repair and growth of nerves.

Previous studies demonstrated that GDAs^{BMP} might be also capable of restricting the glial scar (Hill et al., 2004). However, in our experiment, we could not find evidence to support this. Although the rats that received GDAs^{BMP} showed a trend in behavioral recovery earlier than other groups, no significant changes in Basso Beattie Bresnahan scores occurred after 2 weeks. The reason was that, although GDAs^{BMP} promote the growth of motor and sensory axons into the area around the damage in the early phase after injury, when the axons reach the distal interface, a substantial glial scar has formed in the host tissue. Cell processes of these host astrocytes are disordered and irregular. GDAs^{BMP} lose their linear properties in the border area. As a result, most of the regenerative nerve fibers cannot continue growing across this glial barrier, and axonal terminals twist or form neuromas.

When syringomyelia began to occur 3 days after injury, transplanted GDAs^{BMP} gradually migrated into the corresponding area, and cell proliferation began. This migration filled the cavity effectively, and processes stretched out along the longitudinal axis of the spinal cord, forming the linear channel through which axons could grow. At the same time, GDAs^{BMP} also delayed the expression of inhibitory proteoglycans in the local environment, secreted neuroprotective factors such as brain-derived neurotrophic factor, and stimulated axons growing into the injury center. Although olomoucine prevents proliferation of ordinary astrocytes, GDAs^{BMP} did not lose their characteristics when combined with olomoucine. We observed no differences in the size of the spinal cord cavity between the GDAs^{BMP} and olomoucine + GDAs^{BMP} group at any time point after injury, indicating that the migration, proliferation and differentiation capabilities of GDAs^{BMP} were not affected by the administration of olomoucine. This is probably because of the unique cellular characteristics of the GDAs^{BMP}, and because the action of olomoucine was delayed, as described above. Thus, when olomoucine started to inhibit astrocytes, the GDAs^{BMP} had already filled the injury space.

From 7 days after injury, olomoucine started to regulate and control the glial cell cycle in the damage zone, inhi539-548bit scar tissue formation, and decrease the secretion of harmful factors. However, the proliferation of $GDAs^{BMP}$ was not significantly influenced by olomoucine during this period. The $GDAs^{BMP}$ bridged the injury cavity, and the processes maintained their linear characteristics in the interface of the host tissues to provide axonal growth channels. We have shown in the present study that olomoucine, in combination with $GDAs^{BMP}$ transplantation, notably increases the number of nerve fibers that cross the region of damage and enter the distal interface of host tissues, because olomoucine restricted the formation of glial scar tissue around the cavity. Moreover, hind limb motor function in rats that received olomoucine and $GDAs^{BMP}$ improved consistently throughout the whole observation period, resulting in final Basso Beattie Bresnahan scores that were significantly better than those of rats in the other groups.

Acknowledgments: *We would like to thank the staff in Academy of Military Medical Sciences, and Beijing Institute of Neuroscience, Capital Medical University in China for technical support.*

Author contributions: *Li JJ participated in study design, experimental supervision and financial support. Chen L and Wu L participated in study design, technical support, data acquisition, data analysis and paper drafting. Yang ML participated in study design. Gao F and Yuan L participated in experimental conduction. All authors approved the final version of the paper.*

Conflicts of interest: *None declared.*

References

Akpek EA, Bulutçu E, Alanay A, Korkusuz P, Acaroglu E, Kilinç K, Örs Ü (1999) A study of adenosine treatment in experimental acute spinal cord injury. Effect on arachidonic acid metabolites. Spine (Phila Pa 1976) 24:128-132.

Anderson AJ, Robert S, Huang W, Young W, Cotman CW (2004) Activation of complement pathways after contusion-induced spinal cord injury. J Neurotrauma 21:1831-1846.

Arris CE, Boyle FT, Calvert AH, Curtin NJ, Endicott JA, Garman EF, Gibson AE, Golding BT, Grant S, Griffin RJ, Jewsbury P, Johnson LN, Lawrie AM, Newell DR, Noble ME, Sausville EA, Schultz R, Yu W (2000) Identification of novel purine and pyrimidine cyclin-dependent kinase inhibitors with distinct molecular interactions and tumor cell growth inhibition profiles. J Med Chem 43:2797-2804.

Basso DM, Beattie MS, Bresnahan JC (1995) A sensitive and reliable locomotor rating scale for open field testing in rats. J Neurotrauma 12:1-21.

Bazley FA, Pourmorteza A, Gupta S, Pashai N, Kerr C, All AH (2012) DTI for assessing axonal integrity after contusive spinal cord injury and transplantation of oligodendrocyte progenitor cells. Conf Proc IEEE Eng Med Biol Soc 2012:82-85.

Bramlett HM, Dietrich WD (2007) Progressive damage after brain and spinal cord injury: pathomechanisms and treatment strategies. Prog Brain Res 161:125-141.

Bunge MB (2001) Bridging areas of injury in the spinal cord. Neuroscientist 7:325-339.

Davies JE, Huang C, Proschel C, Noble M, Mayer-Proschel M, Davies SJ (2006) Astrocytes derived from glial-restricted precursors promote spinal cord repair. J Biol 5:7.

Davies SJ, Fitch MT, Memberg SP, Hall AK, Raisman G, Silver J (1997) Regeneration of adult axons in white matter tracts of the central nervous system. Nature 390:680-683.

Ersahin M, Karaaslan N, Gurbuz MS, Hakan T, Berkman MZ, Ekinci O, Denizli N, Aker FV (2011) The safety and diagnostic value of frame-based and CT-guided stereotactic brain biopsy technique. Turk Neurosurg 21:582-590.

Fan C, Zheng Y, Cheng X, Qi X, Bu P, Luo X, Kim DH, Cao Q (2013) Transplantation of D15A-expressing glial-restricted-precursor-derived astrocytes improves anatomical and locomotor recovery after spinal cord injury. Int J Biol Sci 9:78-93.

Fan S, Duba DE, O'Connor PM (1999) Cellular effects of olomoucine in human lymphoma cells differing in p53 function. Chemotherapy 45:437-445.

Fry EJ (2001) Central nervous system regeneration: mission impossible? Clin Exp Pharmacol Physiol 28:253-258.

Gao P, Sun ZS, Wang BM, Li LX, Wang F, Mu LM (2013) Transplantation of neuron-like cells from bone marrow mesenchymal stem cells for treatment of spinal cord injury. Zhongguo Zuzhi Gongcheng Yanjiu 17:4256-4263.

Giménez y Ribotta M, Menet V, Privat A (2001) The role of astrocytes in axonal regeneration in the mammalian CNS. Prog Brain Res 132:587-610.

Glab N, Labidi B, Qin LX, Trehin C, Bergounioux C, Meijer L (1994) Olomoucine, an inhibitor of the cdc2/cdk2 kinases activity, blocks plant cells at the G1 to S and G2 to M cell cycle transitions. FEBS Lett 353:207-211.

Gregori N, Pröschel C, Noble M, Mayer-Pröschel M (2002) The tripotential glial-restricted precursor (GRP) cell and glial development in the spinal cord: generation of bipotential oligodendrocyte-type-2 astrocyte progenitor cells and dorsal-ventral differences in GRP cell function. J Neurosci 22:248-256.

Han X, Yang N, Cui Y, Xu Y, Dang G, Song C (2012) Simvastatin mobilizes bone marrow stromal cells migrating to injured areas and promotes functional recovery after spinal cord injury in the rat. Neurosci Lett 521:136-141.

Hill CE, Brodak DM, Bartlett Bunge M (2012) Dissociated predegenerated peripheral nerve transplants for spinal cord injury repair: a comprehensive assessment of their effects on regeneration and functional recovery compared to Schwann cell transplants. J Neurotrauma 29:2226-2243.

Hill CE, Proschel C, Noble M, Mayer-Proschel M, Gensel JC, Beattie MS, Bresnahan JC (2004) Acute transplantation of glial-restricted precursor cells into spinal cord contusion injuries: survival, differentiation, and effects on lesion environment and axonal regeneration. Exp Neurol 190:289-310.

Hobohm C, Günther A, Grosche J, Roßner S, Schneider D, Brückner G (2005) Decomposition and long-lasting downregulation of extracellular matrix in perineuronal nets induced by focal cerebral ischemia in rats. J Neurosci Res 80:539-548.

Huang K, Sheng WB (2012) Formation of glial scar in the rat spinal cord after injury. Zhongguo Zuzhi Gongcheng Yanjiu 16:3671-3674.

Kakulas BA (1987) The clinical neuropathology of spinal cord injury. A guide to the future. Paraplegia 25:212-216.

Kobayashi NR, Fan DP, Giehl KM, Bedard AM, Wiegand SJ, Tetzlaff W (1997) BDNF and NT-4/5 prevent atrophy of rat rubrospinal neurons after cervical axotomy, stimulate GAP-43 and Talpha1-tubulin mRNA expression, and promote axonal regeneration. J Neurosci 17:9583-9595.

Kuerten S, Gruppe TL, Laurentius L-M, Kirch C, Tary-Lehmann M, Lehmann PV, Addicks K (2011) Differential patterns of spinal cord pathology induced by MP4, MOG peptide 35–55, and PLP peptide 178–191 in C57BL/6 mice. APMIS 119:336-346.

Liu XG, Deng YB, Cai H, Wang LN, Ma YL, Zhang XP, Wei KX (2013a) Transplantation of controlled release glial cell line-derived neurotrophic factor and bone marrow mesenchymal stem cells-derived neuron-like cells reduces myelosyringosis after spinal cord injury. Zhongguo Zuzhi Gongcheng Yanjiu 17:68-73.

Liu XG, Deng YB, Cai H, Zhang XP, Ma YL, Wei KX (2013b) Co-transplantation of controlled release glial cell line-derived neurotrophic factor and bone marrow mesenchymal stem cells-derived neuron-like cells reduces glial scars after spinal cord injury. Zhongguo Zuzhi Gongcheng Yanjiu 17:7427-7434.

Liu Y, Wu Y, Lee JC, Xue H, Pevny LH, Kaprielian Z, Rao MS (2002) Oligodendrocyte and astrocyte development in rodents: An in situ and immunohistological analysis during embryonic development. Glia 40:25-43.

Morgan DO (1995) Principles of CDK regulation. Nature 374:131-134.

Ozdemir M, Attar A, Kuzu I, Ayten M, Ozgencil E, Bozkurt M, Dalva K, Uckan D, Kılıc E, Sancak T, Kanpolat Y, Beksac M (2012) Stem cell therapy in spinal cord injury: in vivo and postmortem tracking of bone marrow mononuclear or mesenchymal stem cells. Stem Cell Rev Rep 8:953-962.

Park DH, Lee JH, Borlongan CV, Sanberg PR, Chung YG, Cho TH (2011) Transplantation of umbilical cord blood stem cells for treating spinal cord injury. Stem Cell Rev Rep 7:181-194.

Parry PV, Engh JA (2012) Promotion of neuronal recovery following experimental SCI via direct inhibition of glial scar formation. Neurosurgery 70:N10-N11.

Phillips A, W, Falahati S, DeSilva R, Shats I, Marx J, Arauz E, Kerr DA, Rothstein JD, Johnston MV, Fatemi A (2012) Derivation of glial restricted precursors from E13 mice. J Vis Exp doi: 10.3791/3462.

Piao JH, Wang Y, Duncan ID (2013) CD44 is required for the migration of transplanted oligodendrocyte progenitor cells to focal inflammatory demyelinating lesions in the spinal cord. Glia 61:361-367.

Schucht P, Raineteau O, Schwab ME, Fouad K (2002) Anatomical correlates of locomotor recovery following dorsal and ventral lesions of the rat spinal cord. Exp Neurol 176:143-153.

Seki T, Hida K, Tada M, Koyanagi I, Iwasaki Y (2002) Graded contusion model of the mouse spinal cord using a pneumatic impact device. Neurosurgery 50:1075-1082.

Sharp J, Frame J, Siegenthaler M, Nistor G, Keirstead HS (2010) Human embryonic stem cell-derived oligodendrocyte progenitor cell transplants improve recovery after cervical spinal cord injury. Stem Cells 28:152-163.

Shechter R, Raposo C, London A, Sagi I, Schwartz M (2011) The glial scar-monocyte interplay: a pivotal resolution phase in spinal cord repair. PLoS One 6:e27969.

Tang X, Davies JE, Davies SJA (2003) Changes in distribution, cell associations, and protein expression levels of NG2, neurocan, phosphacan, brevican, versican V2, and tenascin-C during acute to chronic maturation of spinal cord scar tissue. J Neurosci Res 71:427-444.

Tator CH (1995) Update on the pathophysiology and pathology of acute spinal cord injury. Brain Pathol 5:407-413.

Tian DS, Wang W, Xu YL, Yu ZY, Xie MZ, Wang P, Zhang GB (2006) Effects of cyclin dependent protein kinase inhibitor olomoucine on the microenvironment of axonal regeneration after spinal cord injury: an experiment with rats. Zhonghua Yixue Zazhi 86:901-905.

Tian DS, Xie MJ, Yu ZY, Zhang Q, Wang YH, Chen B, Chen C, Wang W (2007) Effects of the cell cycle inhibitor olomoucine on inflammatory response and neuronal cell death after spinal cord injury in rats. Shenjing Sunshang yu Gongneng Chongjian 2:143-148.

Wang KC, Koprivica V, Kim JA, Sivasankaran R, Guo Y, Neve RL, He Z (2002) Oligodendrocyte-myelin glycoprotein is a Nogo receptor ligand that inhibits neurite outgrowth. Nature 417:941-944.

Wiliams RR, Bunge MB (2012) Schwann cell transplantation: a repair strategy for spinal cord injury? Prog Brain Res 201:295-312.

Wu J, Pajoohesh-Ganji A, Stoica BA, Dinizo M, Guanciale K, Faden AI (2012) Delayed expression of cell cycle proteins contributes to astroglial scar formation and chronic inflammation after rat spinal cord contusion. J Neuroinflammation 9:169.

Xu W, Cheng LM (2013) Neurotrophic factors and spinal cord injury. Zhongguo Zuzhi Gongcheng Yanjiu 17:369-374.

Yazdani SO, Pedram M, Hafizi M, Kabiri M, Soleimani M, Dehghan MM, Jahanzad I, Gheisari Y, Hashemi SM (2012) A comparison between neurally induced bone marrow derived mesenchymal stem cells and olfactory ensheathing glial cells to repair spinal cord injuries in rat. Tissue Cell 44:205-213.

Zhou TJ, Li JJ (2006) Spine and Spinal Cord Injury: Modern Rehabilitation and Treatment. Beijing: People's Medical Publishing House.

Zhang RP, Li JD, Liu Q, Shuang WB, Xie J (2013) Subarachnoid space transplantation of superparamagnetic iron oxide-labeled bone marrow mesenchymal stem cells for treatment of spinal cord injury. Zhongguo Zuzhi Gongcheng Yanjiu 17:74-78.

Zhao ZJ, Sun ZM, Zhang CY, Han JG, Shi RC, Wang WZ (2013) Edaravone combined with neural stem cell transplantation for treatment of spinal cord injury in rats. Zhongguo Zuzhi Gongcheng Yanjiu 17:1862-1867.

Copyedited by Slone-Murphy J, Pack M, Yu J, Qiu Y, Li CH, Song LP, Zhao M